Compensating Small Head Displacements for an accurate fMRI Registration

Diane Lingrand, Johan Montagnat, Louis D. Collins, Jean Gotman

COMPENSATING SMALL HEAD DISPLACEMENTS FOR AN ACCURATE FMRI REGISTRATION

Diane Lingrand, Johan Montagnat, Louis Collins, Jean Gotman

Montréal Neurological Institute - McGill University
3801 rue University, Montréal, QC, Canada, H3A 2B4
{{lingrand,jmontagn,louis}@bic.,jgotma@}mni.mcgill.ca

ABSTRACT

Many medical image processing algorithms require the comparison of multiple scans acquired from a given subject. In the absence of an absolute coordinate system, these different images have to be aligned in a common space before being able to identify similar anatomical landmarks. Several rigid registration techniques have been proposed that estimate the rigid transformation between two anatomical volumes [1] but none of them introduce geometric constraints on the possible position of the human head inside a scanner.

We propose a new method to improve the accuracy of rigid registration in the case of small displacements by restricting the number of degrees of freedom (dof) involved in the registration process. It has been shown in a different context that decreasing the number of dof improves the numerical stability of the displacement recovery algorithm [16, 8] by regularizing the minimized criterion and reducing the number of local minima.

We developed a strategy adapted to the case of human head displacement in a MRI scanner. This algorithm has been successfully tested on 6 sets of fMRI volumes acquired at the MNI on different patients. Each set is composed of 30 to 78 volumes.

1. INTRODUCTION

Linear registration of 3D medical images [1, 2, 5, 9, 6, 15] has been intensively studied over the past decade. Linear registration is used either to align different images in a common space [3, 12], or to correct motion artifacts occurring during longitudinal acquisitions.

While multi-modality or multi-acquisition registration may involve significant displacements as the subject position changes between acquisitions, longitudinal studies usually involve motion with a weak amplitude that are due to breathing motion, heart beat, swallowing, or the difficulty of patients to remain perfectly still for long acquisition periods. Yet, fine measurements of changes in time sequences of noisy images usually require a very precise registration procedure (regions of activity in fMRI sequences, modifications in lesions in MRI sequences, ...).

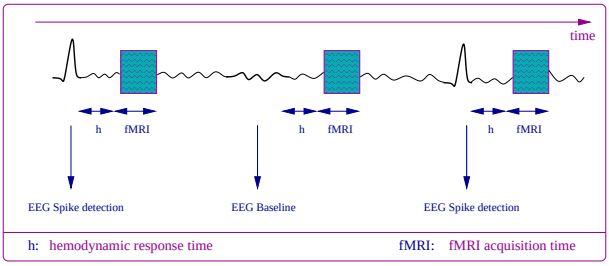

Fig. 1. The EEG signals are continuously observed. Some fMRI volumes acquisitions are triggered when a spike of epileptic activity is detected while some "baselines" are triggered in the absence of epileptic activity.

In this paper we are dealing with fMRI images (functional Magnetic Resonance Imaging) and we focus on the precise registration of brain fMRI images acquired for longitudinal studies of epileptic patients. This is a part of a study on EEG (Electro-EncephaloGraphy) triggered fMRI. The EEG signal acquisitions are continuous and, when a spike of epileptic activity is detected on the EEG signal, one fMRI volume acquisition is triggered. Some baselines events (without any epileptic event) also trigger fMRI volumes for normal cerebral activity detection. This procedure is explained in figures 1 and 2.

The long acquisition time and the annoyance caused by EEG electrodes used for synchronous spike detection often lead to small movements of the patient's head between 3D image acquisitions. These small displacements have to be compensated for prior to statistical study of brain activation regions. However, these motions are constrained by the geometry of the scanner and the anatomy of the body and may yield to constrained displacements.

Registration of 3D medical images has been studied for very different purposes such as computer guided surgery [7] or multi-modality registration [14]. Methods for reducing registration errors have been recently proposed [10]. We propose a new method based on the use of simplified particular cases of motion to improve rigid registration accuracy in longitudinal studies showing small motion artifacts.

The overall idea of our method is to explore particular

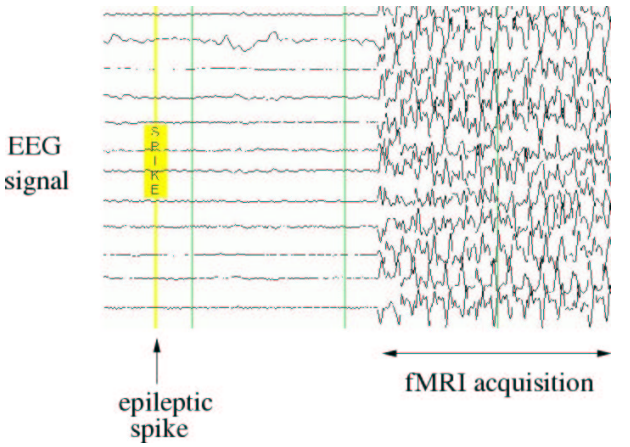

Fig. 2. The EEG signals are continuously monitored. Some fMRI volumes acquisitions are triggered when a spike of epileptic activity is detected. During a fMRI acquisition, the EEG signal is perturbed, as shown above.

displacement cases as opposed to a general rigid transformation between images. Particular cases lead to a reduction in the number of dof for the transformation that allow a better convergence of the optimization procedure involved in rigid registration algorithms. Particular cases have successfully been used to recover 3D motion and camera parameters in the computer vision field [16, 8].

This procedure has been successfully tested on several patients from an EEG triggered fMRI study at the Montréal Neurological Institute.

2. BACKGROUND EQUATIONS

2.1. Rigid displacement equations

A point $\mathbf{M}$ in the world space is moving to the position $\mathbf{M}'$ by a rotation $\mathbf{R}$ and a translation $\mathbf{t}$:

$$\mathbf{M}' = \mathbf{R}\,\mathbf{M} + \mathbf{t}$$

A rigid displacement is parameterized by the rotation $\mathbf{R}$ and the translation $\mathbf{t} = [t_x\ t_y\ t_z]^T$ parameters which are constant in the whole volume. The rotation matrix $\mathbf{R}$ depends only on three parameters $\mathbf{r} = [r_x\, r_y\, r_z]^T$ related to the rotation angle θ and to the rotation axis direction, represented by the unary vector $\mathbf{u}$ by :

$$\mathbf{r} = \theta\,\mathbf{u} \Leftrightarrow \theta = \mathbf{r}$$

A rigid displacement is thus parameterized by 6 parameters corresponding to the 6 degrees of freedom.

Using the notation $\tilde{\mathbf{r}}$ which represents the cross-product operator by $\mathbf{r}$:

$$\tilde{\mathbf{r}} = \mathbf{r} \wedge . = \begin{pmatrix} 0 & -r_z & r_y \\ r_z & 0 & -r_x \\ -r_y & r_x & 0 \end{pmatrix}$$

the rotation matrix $\mathbf{R}$ is expressed as : $\mathbf{R} = e^{\tilde{\mathbf{r}}}$. The reader can easily verify that $\mathbf{R}$ is a rotation matrix ($\mathbf{R}\,\mathbf{R}^T = \mathbf{I}$ and $\det \mathbf{R} = +1$). Since $\tilde{\mathbf{r}}^3 = -\theta\,\tilde{\mathbf{r}}$, the decomposition of the exponential can be rewritten in a simple way, using the Rodrigues formula, [13] :

$$\mathbf{R} = \mathbf{I} + \frac{\sin\theta}{\theta}\,\tilde{\mathbf{r}} + \frac{1-\cos\theta}{\theta^2}\,\tilde{\mathbf{r}}^2 \qquad (1)$$

If we consider the vector $\rho = 2\,\tan(\frac{\theta}{2})\mathbf{u}$, we can verify that this new parameterization lead to a rational formulation of the Rodrigues formula 1 :

$$\mathbf{R} = \mathbf{I} + \left[\frac{\tilde{\rho} + \frac{1}{2}\,\tilde{\rho}^2}{1 + \frac{\rho^T\cdot\rho}{4}}\right] \qquad (2)$$

and we have :

$$\begin{cases} \theta &= 2\,\arctan\left(\frac{\|\rho\|}{2}\right) \\ trace(\mathbf{R}) &= \frac{12-\|\rho\|^2}{4+\|\rho\|^2} \Rightarrow \|\rho\|^2 = 4\,\frac{3-trace(\mathbf{R})}{1+trace(\mathbf{R})} \end{cases}$$

The benefit of this formulation is twofold : rational equations leads to more precise numeric computations and, the inverse equations are also simpler :

$$\begin{cases} \rho_x = \lambda\,(R_{32} - R_{23}) \\ \rho_y = \lambda\,(R_{13} - R_{31}) \\ \rho_z = \lambda\,(R_{21} - R_{12}) \end{cases}$$

with $\lambda = \frac{1}{2}\,(1 + \frac{\|\rho\|^2}{4}) = \frac{2}{1+trace(\mathbf{R})}$

During fMRI acquisition, the patient try to move as little as possible, however they still move. If the angle of rotation of these unwanted displacement is small enough, the rotation may be approximated by its first order expansion:

$$\mathbf{R} = e^{\tilde{\mathbf{r}}} = \mathbf{I} + \tilde{\mathbf{r}} + o(\tilde{\mathbf{r}}) = \begin{pmatrix} 1 & -r_z & r_y \\ r_z & 1 & -r_x \\ -r_y & r_x & 1 \end{pmatrix}$$

The inverse transformation is trivial.

2.2. Particular cases of displacement

We are interested in the rigid part of volume registration. Other non rigid deformations are not taken into account because we are dealing with only one patient at the same time (the skull is rigid) and one image modality (no scales and shears). As a generally accepted hypothesis, we will consider that there is no head displacement during one volume acquisition, which lasts approximately 2 seconds. In this part, we will study the equations of rigid displacement and their singularities.

A subject lying down in the scanner has the head approximately fixed by a head coil as shown in figure 3. It is still possible to move but with a small amplitude and often not along all 6 degrees of freedom. The displacements are mostly small rotations around an axis passing near the

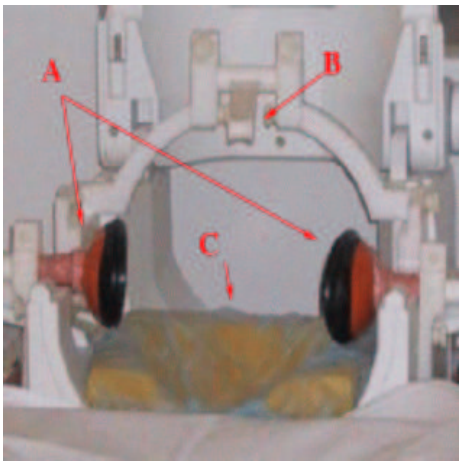

Fig. 3. Head coil in the Siemens scanner. **A** stabilizes the ears positions, **B** the nose and **C**, the head coil stabilizes the head back.

head center. The mislocalization of the center of reference is responsible of the translation components.

Since we are interested in particular directions of the rotation axis, we will consider the **r** vector to have or not to have one or several null components. We show in table 1 three sets of cases that we will study in this paper. The first set corresponds to different cases of translation direction, the second to the rotation mode (no rotation, small rotation, general rotation) and the last set to different cases of rotation axis. A particular case of motion is composed by a particular case of each label set.

A particular case is called "**ti**$\mathbf{R}$**ju**k" where the indices i, j and k correspond to the values in table 1. Since in case of no rotation (**R1**) we do not care about the rotation axis, we will consider the following values of indices : $i \in [1;8]$, $j \in [1;3]$ and, if $j = 1$ then $k = 1$ else $k \in [1;7]$. We thus have $8 * (1 * 1 + 2 * 7) = 120$ different particular cases.

2.3. The registration process

We have implemented our method in the *autoreg*[1] package developed by Collins *et al*[3] for linear and non-rigid registration of brain images. The algorithm is based on a simplex optimization procedure that minimizes an objective function [4] measuring the similarity between a resampled source image and a target image. A cross correlation measure is used in the case of fMRI registration [11].

The simplex optimization procedure minimizes the value of the fit value r associated to a transformation between two volumes. This fit value is defined by :

$$r = \frac{f_1}{\sqrt{f_2} * \sqrt{f_3}}$$

[1] http://www.bic.mni.mcgill.ca/software/mni_autoreg/

label	constraints	displacement
t1	$t_x = t_y = t_z = 0$	no translation
t2	$t_x = t_y = 0$	translation on z-axis
t3	$t_x = t_z = 0$	translation on y-axis
t4	$t_y = t_z = 0$	translation on x-axis
t5	$t_x = 0$	translation $\perp$ x-axis
t6	$t_y = 0$	translation $\perp$ y-axis
t7	$t_x = 0$	translation $\perp$ z-axis
t8	$\varnothing$	general translation
R1	$\mathbf{R} = \mathbf{I}$	null rotation
R2	$\begin{cases} \mathbf{R} = \mathbf{I} + \tilde{\mathbf{r}} \\ \mathbf{r} = \theta\, \mathbf{u} \end{cases}$	first order
R3	$\begin{cases} \mathbf{R} = \mathbf{I} + \left[\frac{\tilde{\rho} + \frac{1}{2}\tilde{\rho}^2}{1 + \frac{\rho^T \rho}{4}}\right] \\ \rho = 2 \tan \frac{\theta}{2}\, \mathbf{u} \end{cases}$	general case
u1	$u_x = u_y = 0$	z rotation axis
u2	$u_x = u_z = 0$	y rotation axis
u3	$u_y = u_z = 0$	x rotation axis
u4	$u_x = 0$	rotation axis $\perp$ x-axis
u5	$u_y = 0$	rotation axis $\perp$ y-axis
u6	$u_z = 0$	rotation axis $\perp$ z-axis
u7	$\varnothing$	general rotation

Table 1. Particular cases of displacements : translation direction, rotation mode and rotation axis.

where :

$$\begin{cases} f_1 = \sum d_1 * d_2 \text{ (point to point multiply)} \\ f_2 = \sum d_1^2 \text{ (sum of all points squared)} \\ f_3 = \sum d_2^2 \text{ (sum of all points squared)} \end{cases}$$

The fit value is normalized between 0 and 1. The ideal registration gives a fit value of 1.

As an initial guess of displacement, we took the identity transformation. Considering that the motion estimation is better when we have a reasonable guess for the center of rotation since it makes the parameters more orthogonal to each other (e.g. a small change in rotation will not grossly affect the translations), we choose the center of gravity of the head.

We embedded the rigid displacement estimation process in a loop that examines all particular cases of displacements and, for each case, estimates the underlying parameters of the simplified model. After this loop, the case that generates the best fit value is selected.

3. EXPERIMENTS

3.1. Data used

We used fMRI volumes acquired during EEG triggered fMRI experiments on a 1.5 Tesla Siemens Vision scanner, using gradient echo EPI sequences. We used data from four patients which were selected because of drug resistance and

name	number of volumes
Charlie Brown1	74
Charlie Brown2	35
Charlie Brown3	30
Snoopy	66
Linus	78
Woodstock	48

Table 2. Number of data acquired for each patient. We have two sets of data for Charlie Brown who went three times in the scanner.

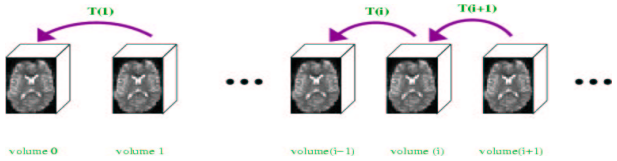

Fig. 4. Registration with respect to the previous volume. $T(i)$ is the transformation to apply on volume(i) for registration with respect to volume(i-1).

focal epilepsy : Charlie Brown, Snoopy, Linus and Woodstock. For each patient, EEG electrodes were placed on the scalp and acquisition of an fMRI volume was triggered by epileptic activities detection. Some volumes are also acquired in the absence of epileptic activity (baselines) in order to determine a reference for epileptic activity localization (see figures 1 and 2). Since Charlie Brown has been scanned three times, we have three data sets for this patient. The number of fMRI volumes we acquired for each patient is collected in table 2. The acquisition of volumes is not continuous (there might be several seconds or minutes between two acquisitions) but the patient remains in the scanner during the whole study (which takes less than 1h30). Each volume is composed of 25 slices 64*64 each. The voxels dimension is 5*5*5 mm^3. The acquisition of a single volume takes a few seconds.

3.2. Between two consecutives volumes, particular cases occur frequently.

In this experiment, we identify the transformation between each volume and the previous one as shown in figure 4. For each pair of frames, we try all cases of rigid displacement seen in table 1 and select the result of best fit value.

Concerning the registration between two consectives volumes, particular cases often give better result (and never worse) and the mean improvement is significant. We show in figures 5 to 10 the improvement brought by the particular approach. The value Δ displayed represents the relative improvement of the particular case compared to the general

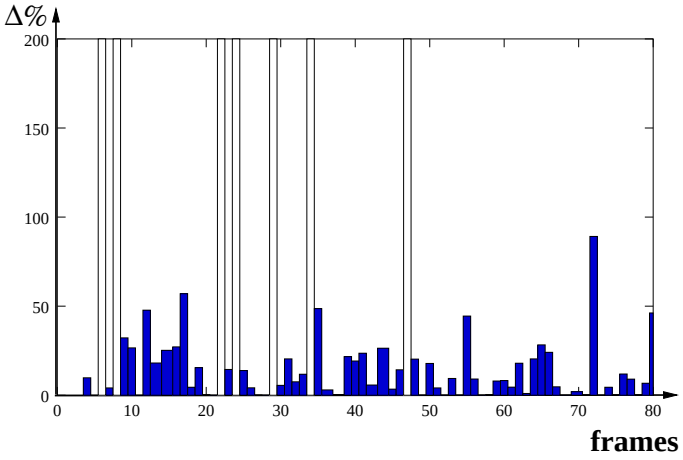

Fig. 5. Δ values for each volume from equation 3. Measurement of the particular cases approach in the case of registration of one volume with respect to the previous one. This example shows, for patient Charlie Brown1, that our method increase the accuracy of parameters estimation. The mean improvement is 15 % with standard deviation 17.

method. This is obtained by :

$$\Delta = \frac{\text{general case fit value} - \text{best case fit value}}{\text{identity fit value} - \text{general case fit value}} \quad (3)$$

This value may be unstable when there is no displacement because of the nullity of the denominator. In the following experiments, we will not take the values of Δ greater than 150 % (white bars) into account.

For each volume, we give the degrees of freedom in figures 11 to 16. The value 6 corresponds to 3 degrees of freedom in rotation and 3 in translation. The rotation may be general or approximated to its first order.

We have experimented 323 registrations, each with 120 different particular cases. We observed that, among these 120 different cases, only 63 were selected, meaning that some may not occur in practice. The general case was selected 43 times, the first order of rotation with 6 dof 67 times, and the others, less than 20 times. This preliminary result could be useful in order to reduce the number of cases to test, and thus, reduce the computational cost. Furthermore, it could be interesting to study, for a volume to be registered with respect to another, if some cases are equivalent regarding the fit value. This would allow to select only few cases among the 120.

The interest of using a first order development of the rotation is demonstrated by the fact that, considering the 323 registrations, first order rotation was selected 204 times, general rotation 111 times and null rotation 8 times.

4. CONCLUSION

In this paper, we presented an adapted strategy to compensate for head small displacements in a scanner. The ap-

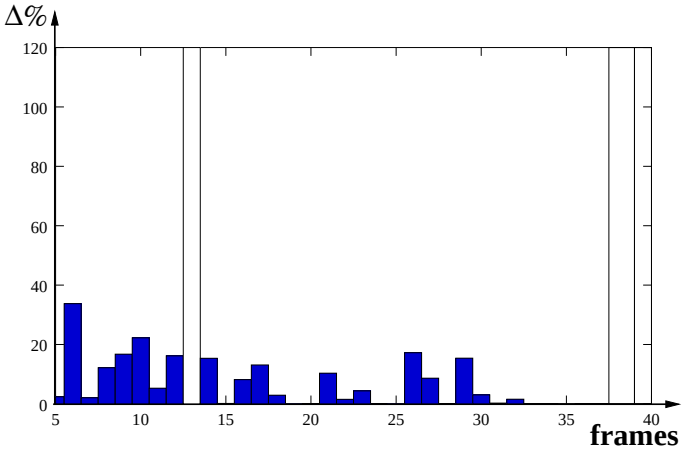

Fig. 6. The same as figure 5 for patient Charlie Brown2. The mean improvement is 12 % with standard deviation 24.

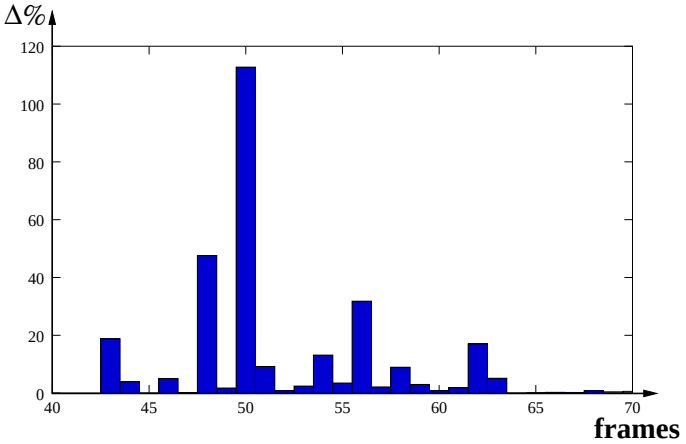

Fig. 7. The same as figure 5 for patient Charlie Brown3. The mean improvement is 11 % with standard deviation 23.

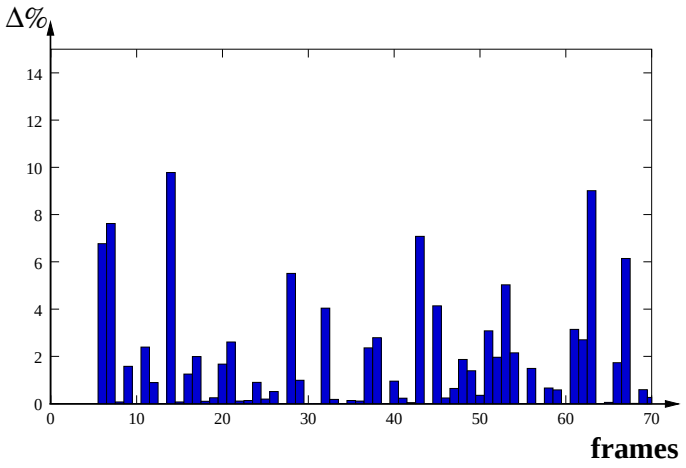

Fig. 8. The same as figure 5 for patient Snoopy. The mean improvement is 2 % with standard deviation 2.

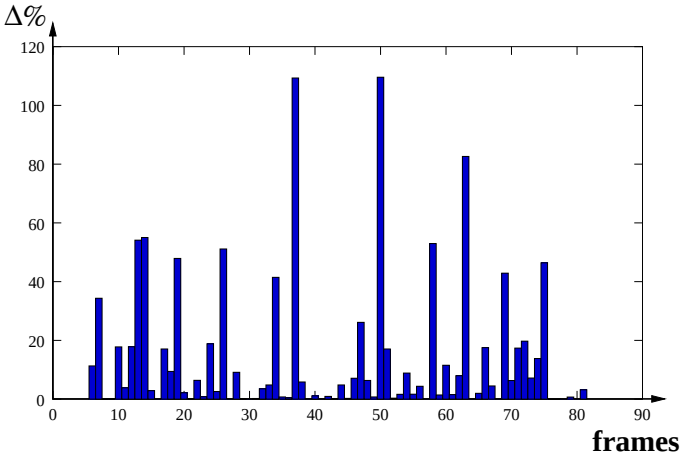

Fig. 9. The same as figure 5 for patient Linus. The mean improvement is 15 % with standard deviation 24.

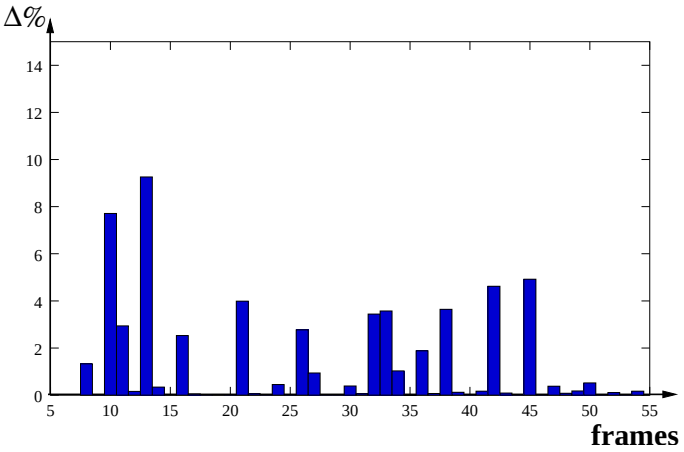

Fig. 10. The same as figure 5 for patient Woodstock. The mean improvement is 1.4 % with standard deviation 2.

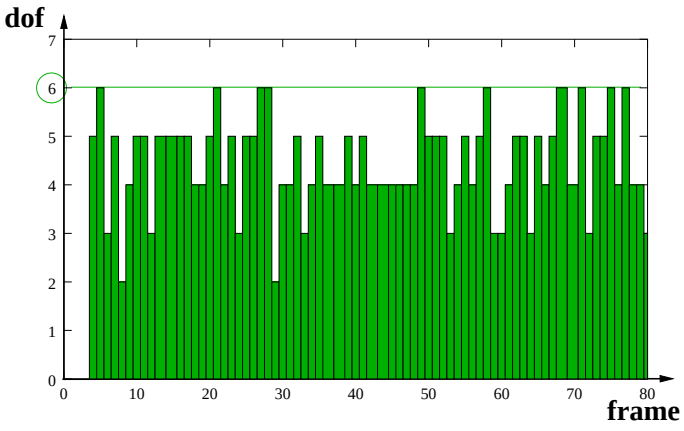

Fig. 11. Degrees of freedom of best case for each volume in the case of registration of one volume with respect to the previous one. The value 6 corresponds to 3 dof in rotation and 3 dof in translation. This example shows, for patient Charlie Brown1, that there is often less than 6 dof. The mean dof is 4.5 with a standard deviation of 1.0

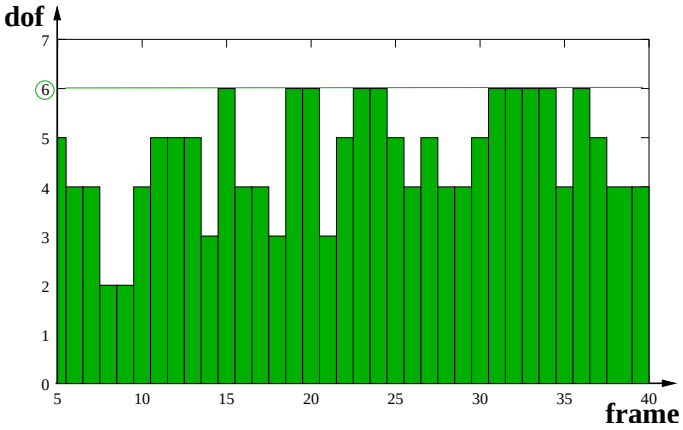

Fig. 12. The same as figure 11 for patient Charlie Brown2. The mean dof is 4.6 with a standard deviation of 1.1

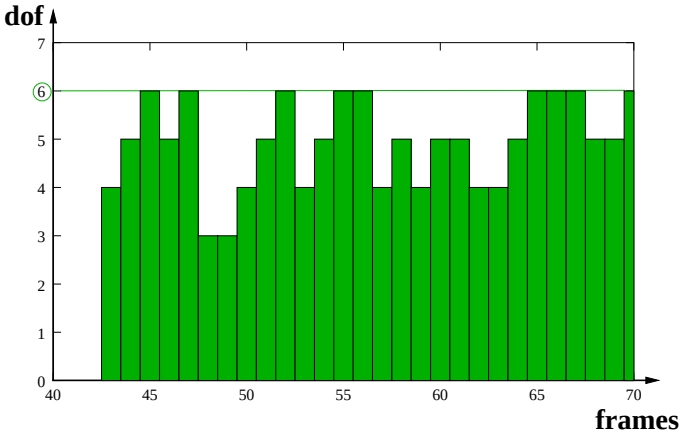

Fig. 13. The same as figure 11 for patient Charlie Brown3. The mean dof is 4.9 with a standard deviation of 0.9

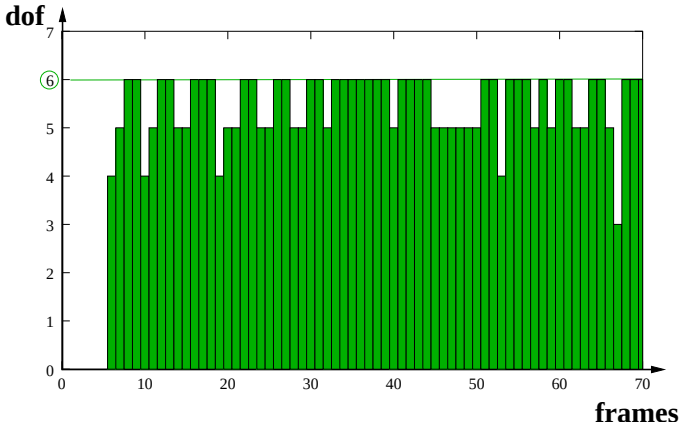

Fig. 14. The same as figure 11 for patient Snoopy. The mean dof is 5.5 with a standard deviation of 0.7

Fig. 15. The same as figure 11 for patient Linus. The mean dof is 4.6 with a standard deviation of 1.1

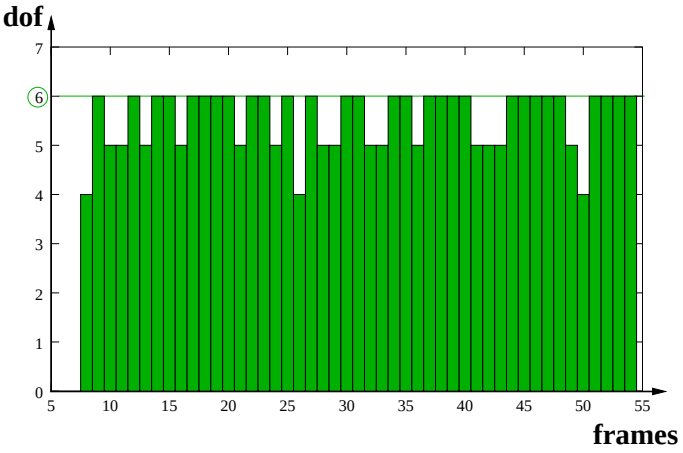

Fig. 16. The same as figure 11 for patient Woodstock. The mean dof is 5.6 with a standard deviation of 0.6

proach was tested on several sets of fMRI volumes. The experimental results show an improvement of the registration accuracy in most cases. Between two frames, particular cases occur frequently. We observed also that some cases studied never occur in practice.

The strategy described here is not dependent of the acquisition procedure and can obviously be applied to other image modalities.

This study could be extended in different ways. First, a clinical trial involving a larger amount of subjects would confirm whether it is possible to withdraw some particular cases. Second, the results could be refined by identifying the particular cases that arise from the specific geometry of the head coil (flat, spherical, ...).

Acknowledgments

Thanks go to all people at the Brain Image Center and the EEG team of the MNI for their welcoming, kindness and fruitful discussions.

5. REFERENCES

[1] L.G. Brown. A Survey of Image Registration Techniques. *ACM Computing Surveys*, 24(4):325–376, December 1992.

[2] A. Collington, F. Maes, D. Delaere, D. Vandermeulen, P. Suetens, and Marchal G. Automated multi-modality image registration based on information theory. In *Proc. Information Processing in Medical Imaging*, pages 263–274, Brest, France, June 1995.

[3] D. L. Collins, P. Neelin, T. M. Peters, and A. C. Evans. Automatic 3D Inter-Subject Registration of MR Volumetric Data in Standardized Talairach Space. *Journal of Computer Assisted Tomography*, 18(2):192–205, 1994.

[4] D.L. Collins and A.C. Evans. ANIMAL: validation and applications of nonlinear registration-based segmentation. *Int. Journal of Pattern Recognition and Artificial Intelligence*, 8(11):1271–1294, 1997.

[5] K. Friston, J. Ashburner, Frith C., and J.B. Poline. Spatial registration and normalization of images. *Human Brain Mapping*, 2(1):1–25, 1995.

[6] Y. Ge, J. Fitzpatrick, R. Kessler, and R. Margolin. Intersubject brain image registration using both cortical and subcortical landmarks. In *Proc, SPIE Medical Imaging*, volume 2434, pages 81–95, 1995.

[7] S. Lavallée. *Registration for computer integrated surgery: methodology, state of the art*. MIT Press, 1995.

[8] D. Lingrand. Particular Forms of Homography Matrices. In *BMVC 2000*, volume 2, pages 596–605, 2000.

[9] A. Maintz and M. Vierveger. A survey of medical image registration. *Medical Image Analysis*, 2(1):1–36, 1998.

[10] S. Ourselin, A. Roche, S. Prima, and N. Ayache. Block Matching: a General Framework to Improve Robustness of Rigid Registratoin of Medical Images. In *Medical Image Computing and Computer-Assisted Intervention (MICCAI'00)*, LNCS, Pittsburgh, USA, October 2000. Springer.

[11] G.P. Penney, J. Weese, J.A. Little, P. Desmedt, D.LG. Hill, and D.J. Hawkes. A Comparison of Similarity Measures for Use in 2D-3D Medical Image Registration. In *Medical Image Computing and Computer-Assisted Intervention (MICCAI'98)*, volume 1496 of *LLNCS*, pages 1153–1161, Cambridge, USA, October 1998. Springer.

[12] A. Roche, X. Pennec, M. Rudolph, D.P. Auer, G. Malandain, S. Ourselin, L.M. Auer, and N. Ayache. Generalized Correlation Ratio for Rigid Registration of 3D Ultrasound with MR Images. In *Medical Image Computing and Computer-Assisted Intervention (MICCAI'00)*, Lecture Notes in Computer Science, Pittsburgh, USA, October 2000. Springer.

[13] O. Rodrigues. Des lois géométriques qui régissent les déplacements d'un système solide dans l'espace, et de la variation des coordonnées provenant de ces déplacements considérés indépendamment des causes qui peuvent les produire. *Journal de Mathématiques Pures et Appliquées*, 5, 1840. pp. 380–440.

[14] C. Studholme, D.L.G. Hill, and D.J. Hawkes. Automated 3-D registration of MR and CT images of the head. *Medical Image Analysis*, 2(1):163–175, 1996.

[15] J. Talairach and P. Tournoux. *Co-planar Stereotaxic Atlas of the Human Brain: 3-Dimensional Proportional System. An Approach to Cerebral Imaging.* Georg Thieme Verlag, New York, 1988.

[16] T. Viéville and D. Lingrand. Using specific displacements to analyze motion without calibration. *International Journal of Computer Vision*, 31(1):5–29, 1999.